

Dynamics of hydrological model parameters: calibration and reliability

Tian Lan¹, Kairong Lin^{1,2,3}, Xuezhi Tan^{1,2,3}, Chong-Yu Xu⁴, Xiaohong Chen^{1,2,3}

¹Center for Water Resources and Environment, Sun Yat-sen University, Guangzhou, 510275, China.

²Guangdong Engineering Technology Research Center of Water Security Regulation and Control for Southern China, Guangzhou 510275, China.

³School of Civil Engineering, Sun Yat-sen University, Guangzhou, 510275, China.

⁴Department of Geosciences, University of Oslo, P.O. Box 1047, Blindern, 0316 Oslo, Norway

Correspondence to: Kairong Lin (linkr@mail.sysu.edu.cn)

Contents of this file

1 Case study and data

2 HYMOD model

3 SCE-UA

4 Violin plot

5 Multi-metric evaluation

6 Evaluation of sub-period calibration schemes in Mumahe basin and Xunhe basin

7 Convergence performance in Mumahe basin and Xunhe basin using ECP-VP

References

Introduction

This supporting information includes eight sections that support the analysis. The *1 Case study and data* section is used to support the *2 Background* section in the main manuscript. The *2 HYMOD model* section is used to support the *3.1 Sub-period calibration* section in the main manuscript. The *3 SCE-UA algorithm* section and *4 Violin plot* section are used to support the *3.2 A tool for reliability evaluation* section in the main manuscript. The *5 Multi-metric evaluation* section and *6 Evaluation of sub-period calibration schemes in Mumahe basin and Xunhe basin* section are used to account for *4.1 Evaluation of calibration schemes* section in the main manuscript. The *7 Convergence performance in Mumahe basin and Xunhe basin using ECP-VP* section is used to supplement *4.3 Evaluation of reliability* section in the main manuscript.

1 Case study and data

In this study, three sub-basins with different spatial scales in the Hanjiang Basin, i.e., Hanzhong basin, Mumahe basin, and Xunhe basin, were selected as case study to demonstrate the proposed approach. The Hanjiang River is the largest tributary of the Yangtze River in China. It is the headwater of the middle route of the South-to-North Water Transfer Project in China (SNWTP) and plays an important role in the water supply for northern China, as illustrated in Figure 1 in the main manuscript. Climatically, the Hanjiang basin is located in the monsoon region of East Asia subtropical zone. Summer is the main flooding season for the Hanjiang basin due to the heavy monsoon rainfall. Temporal distributions of the rain and temperature zones are affected by the seasonal motion of subtropical highs. Evaporation also has seasonal fluctuation with the highest values in summer and the lowest values in winter (Lin et al., 2010). It is cold and dry in winter and is warm and humid in summer. Such variations are synchronous with the seasonal changes in vegetation density and types (Fang et al., 2002). Subtropical vegetation affects the temporal distributions of the moisture conditions. Therefore, the three sub-basins in the Hanjiang basin are ideal places for studying seasonal calibrations. The significant intra-annual changes in the climate and land-surface conditions provide a chance to explore the seasonal dynamics of the hydrological processes. The geographical properties in these three case studies are briefly introduced as follows. The Hanzhong basin has a drainage area of 9329 km² and is located in the upper reaches of the Hanjiang River. The basin is bordered to the southwest by the Chengdu Plain, to the north by the Wei River valley, and to the south by the Middle Yangtze region. Hence, this basin is an important center for the communication networks between different regions in China (Chen et al., 2016; Sun et al., 2012). The Mumahe basin has a drainage area of 1224 km². It is the largest basin on the south bank of the Hanjiang River. Low hills and moderate slopes characterize the topography of the Mumahe basin (Lin et al., 2010). Xunhe basin has a drainage area of 6448 km². In this basin, mountains dominate the topography and the elevations of the mountain peaks range from 2000 m to 3000 m (Lin et al., 2010; Li et al., 2016). Daily streamflow and climatic data from 1980 to 1990 are used. Nearly 73% of the data samples (1980–1987) is used for calibration and the remainder (1988-1990) is utilized to verify the developed model.

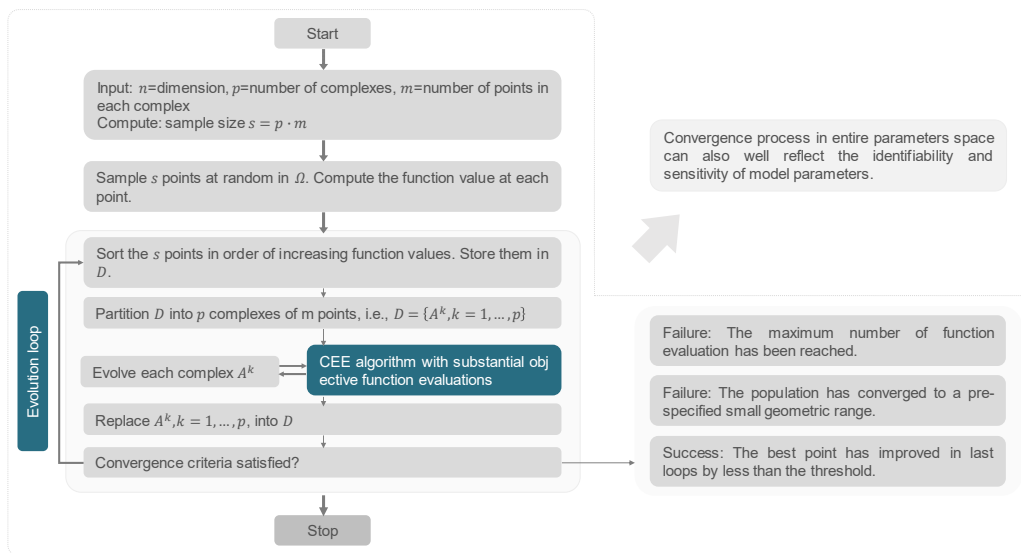
2 HYMOD model

The HYMOD model (Moore, 1985; Wagener et al., 2001; Vrugt et al., 2002; Yadav et al., 2007; De Vos et al., 2010; Pathiraja et al., 2018) consists of a simple rainfall excess model based on the probability-distributed moisture store which characterizes the catchment storage as a Pareto distribution of buckets of varying depth as the soil moisture accounting component. It routes through three parallel tanks for quick flow and a tank for slow flow and required five adjustable parameters: H_{UZ} , B , α , K_q and K_s . XH_{UZ} and XC_{UZ} are state variables characterizing the upper soil moisture content; AE is actual evapotranspiration which is calculated by linear correlations between the soil moisture state and the potential evapotranspiration; $effP$ is effective precipitation; OV is excess precipitation to routing module generated from overflow of soil moisture accounting component;

See (Moore, 1985) for a detailed description of the soil moisture accounting model; X_{q1} , X_{q2} , X_{q3} and X_s are the state variables of the individual tanks of the routing module; Q_q and Q_s are the flow values generated from the quick- and slow-flow tanks, respectively.

3 SCE-UA

- 5 The shuffled complex evolution approach (SCE-UA), as an effective global optimization method, is a commonly used algorithm, because it is open source and was the first algorithm aimed specifically at calibrating hydrological models (Khakbaz and Kazeminezhad, 2012; Eckhardt and Arnold, 2001; Duan et al., 1994; Sorooshian et al., 1993). The technical details about the SCE-UA can be shown in the flowchart (see Figure S1) (Duan et al., 1994). In the SCE-UA, the upper limit of the objective function evaluation is set to 10,000 times. All other settings of the SCE-UA technique are the default.



10

Figure S1. The flowchart of the SCE-UA algorithm (Duan et al., 1994; Duan et al., 1993; Duan et al., 1992).

4 Violin plot

- A violin plot is a combination of a Box Plot and a Density Plot showing more details of data distribution. As shown in Figure S2, the thick black bar in the center represents the interquartile range. The white dot represents the median. The thin black line is extended from the thick black bar and represents the 95% confidence intervals. On each side of the thin black line is a kernel density estimation to show the distribution shape of the data. Wider sections of the violin plot represent a higher probability that members of the population will take on the given value; the skinnier sections represent a lower probability (Hintze and Nelson, 1998). The violin plots can exactly show the kernel density distribution, avoiding the overlapping traditional density plot occur to become difficult to identify. Moreover, unlike bar graphs with means and error bars, violin plots contain all data
- 15

points, which makes them an excellent tool to visualize samples of small sizes. Violin plots are perfectly appropriate even if your data do not conform to normal distribution. They work well to visualize both quantitative and qualitative data.

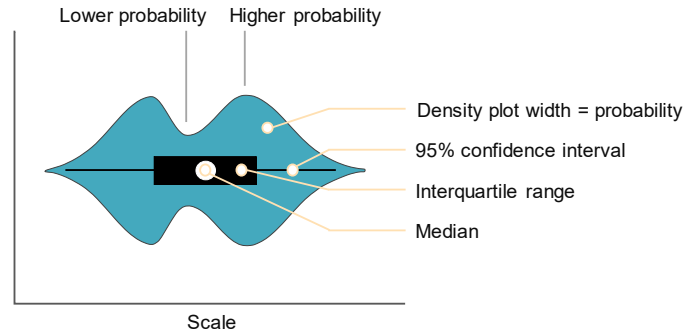


Figure S2. Anatomy of a violin plot

5 Multi-metric evaluation

A multi-metric framework is conducted to assess the prediction accuracy of various flow conditions. The metrics incorporate the NSE, the NSE of the logarithmic streamflow (LNSE), and a five-segment flow duration curve (5FDC) with the RMSE. Their detailed descriptions are briefed in Table S1. The five-segment flow duration (5FDC) with RMSE is proposed by (Pfanterstill et al., 2014). For flow duration curve (FDC), it is usually split into different segments to describe different flow characteristics of a catchment, markedly well in very high or very low segment (Cheng et al., 2012;Coopersmith et al., 2012;Kim and Kaluarachchi, 2014;Pugliese et al., 2014;Pfanterstill et al., 2014). Although FDC represents only the distribution, or statistical metrics of flow levels occurred throughout the records without any information on accurate flow timing, the FDC gives the possibility to analyze the deficits in volume prediction (Pfanterstill et al., 2014). The RMSE with quadratic character is usually used to evaluate the poor model performance due to strong sensitivity to extreme positive and negative error values. Therefore, we apply the 5FDC with RMSE to analyzing the performance of the model runs in the different parts (very low, low, medium, high and very high flow phases) of the hydrograph.

Table S1. Definitions of the performance metrics for the 5FDC.

Performance metric	Description
NSE	Sensitive to peaks and discharge dynamic
LNSE	Emphasizing low flows with log of discharge
RMSE_Q5	RMSE in FDC Q5 very low segment volume
RMSE_Q20	RMSE in FDC between Q5 and Q20 low segment volume
RMSE_Qmid	RMSE in FDC between Q20 and Q70 mid segment volume
RMSE_Q70	RMSE in FDC between Q70 and Q95 high segment volume
RMSE_Q95	RMSE in FDC Q95 very high segment volume

6 Evaluation of sub-period calibration schemes in Mumahe basin and Xunhe basin

Table S2. Evaluation results of the multi-metric framework for Scheme 0 and Scheme 4 performance in the Mumahe basin. Scheme 0: WPCS; Scheme 4: PCSP. The best performance is marked red.

	NSE	LNSE	RMSE_Q5	RMSE_Q20	RMSE_mid	RMSE_Q70	RMSE_Q95
Calibration							
Scheme 0	0.691	0.445	0.953	0.357	0.118	0.554	0.909
Scheme 4	0.324	0.262	0.362	0.070	0.112	0.288	0.729
Verification							
Scheme 0	0.750	0.686	1.082	0.342	0.183	0.825	1.450
Scheme 4	0.345	0.325	0.338	0.056	0.165	0.524	0.717
Calibration-verification							
Scheme 0	0.059	0.241	0.129	-0.015	0.065	0.271	0.541
Scheme 4	0.021	0.062	-0.023	-0.013	0.053	0.236	-0.013

Table S3. The optimal parameter sets for Scheme 0 and Scheme 4 performance in the Mumahe basin. Scheme 0: WPCS; Scheme 4: PCSP.

5

		H_{uz}	B	alpha	K_q	K_s
Scheme 0		916.692	1.990	0.048	1.000	0.079
Scheme 4	Dry period	999.540	1.990	0.051	0.501	0.038
	Rainfall period I	999.998	1.900	0.010	0.713	0.143
	Rainfall period II	27.799	1.990	0.010	0.801	0.237
	Rainfall period III	644.639	1.990	0.010	0.501	0.090

Minimum  Maximum

Table S4. Evaluation results of the multi-metric framework for five sub-period calibration-verification schemes performance in the Xunhe basin. Scheme 0: WPCS; Scheme 4: PCSP. The best performance is marked red.

	NSE	LNSE	RMSE_Q5	RMSE_Q20	RMSE_mid	RMSE_Q70	RMSE_Q95
Calibration							
Scheme 0	0.617	0.334	0.495	0.164	0.304	0.192	0.573
Scheme 4	0.252	0.183	0.165	0.153	0.157	0.166	0.724
Verification							
Scheme 0	0.683	0.478	0.616	0.271	0.322	0.091	0.674
Scheme 4	0.253	0.258	0.186	0.071	0.076	0.092	0.292
Calibration-verification							
Scheme 0	0.066	0.144	0.120	0.107	0.018	-0.100	0.101
Scheme 4	0.001	0.074	0.021	-0.055	-0.081	-0.074	-0.432

Table S5. The optimal parameter sets for five sub-period calibration schemes in the Xunhe basin. Scheme 0: WPCS; Scheme 1: SCSW; Scheme 4: PCSP. The best performance is marked red.

		H_{uz}	B	alpha	K_q	K_s
Scheme 0		999.991	1.259	0.342	0.894	0.024
Scheme 4	Dry period	999.943	0.391	0.565	0.506	0.011
	Rainfall period I	988.154	1.602	0.031	1.000	0.112
	Rainfall period II	353.777	0.641	0.010	0.500	0.319
	Rainfall period III	456.369	0.418	0.104	1.000	0.121



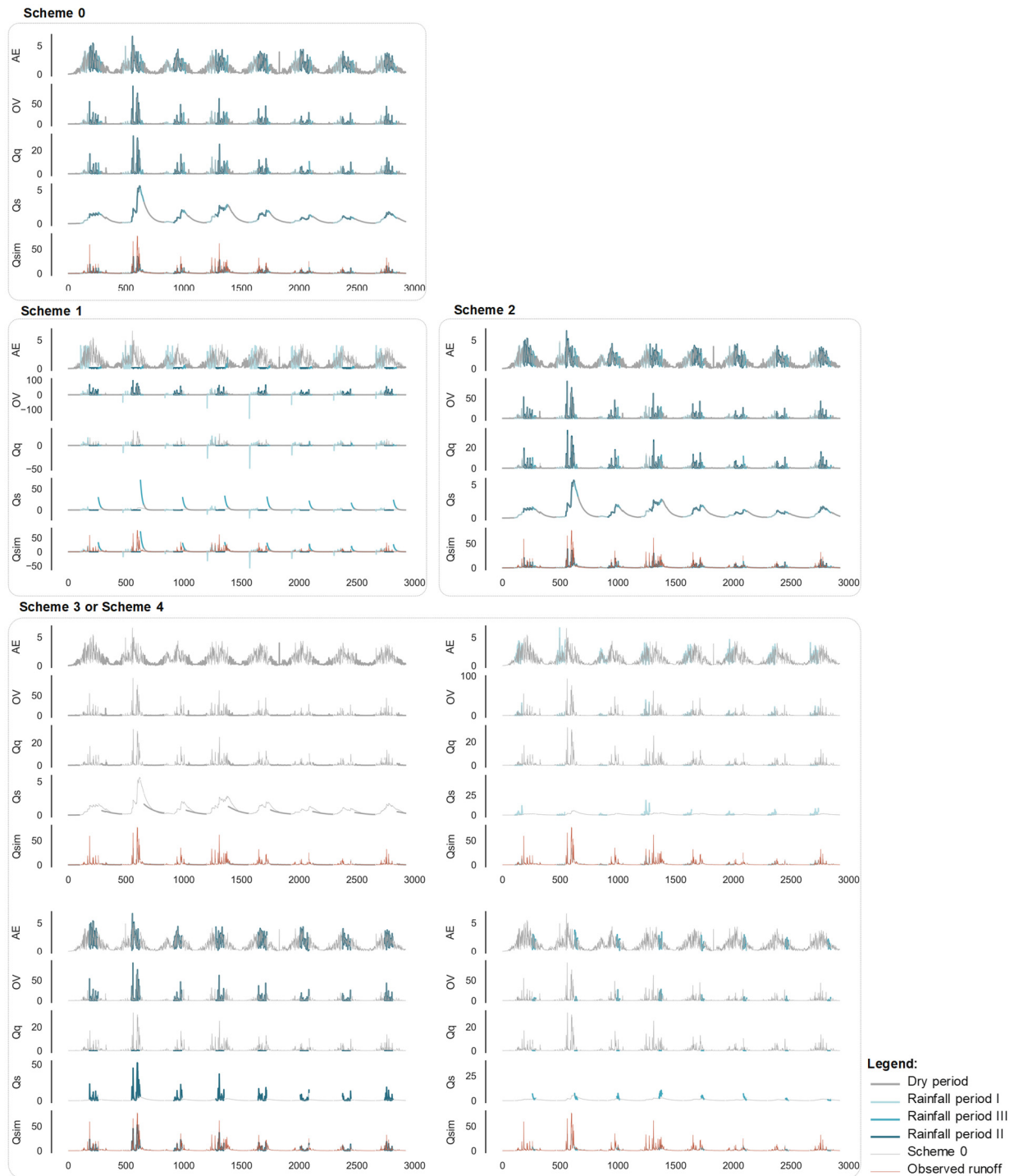


Figure S3. All fluxes (including AE , OV , Q_q , Q_s , and Q_{sim}) for five schemes in the whole calibration period in Hanzhong basin. The thin grey lines denote the simulated fluxes time series in Scheme 0. The red lines denote the observed streamflow time series.

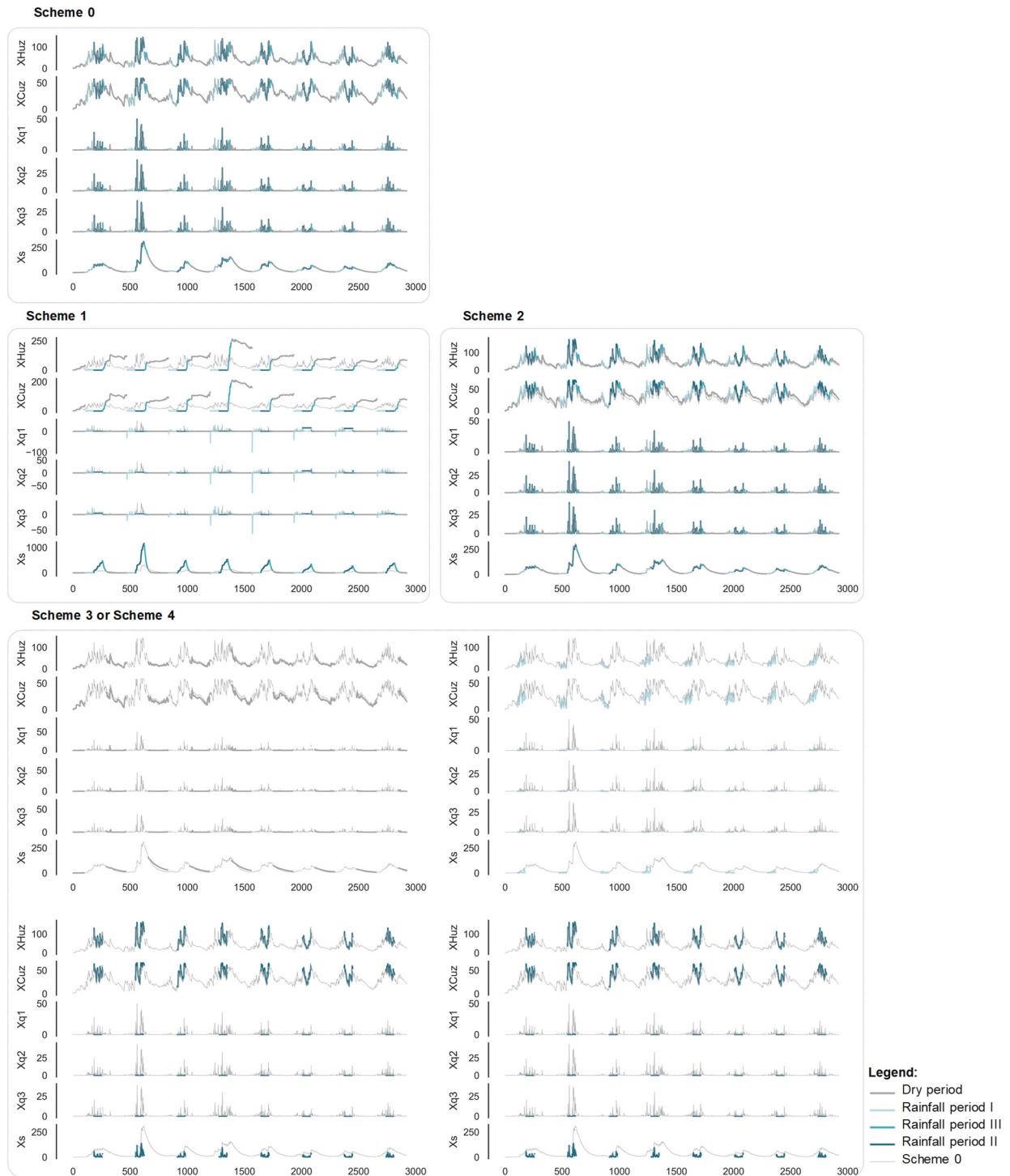


Figure S4. All state variables (including XH_{UZ} , XC_{UZ} , X_{q1} , X_{q2} , X_{q3} , and X_s) for five schemes in the whole calibration period in Hanzhong basin. The thin grey lines denote the simulated state variables time series in Scheme 0.

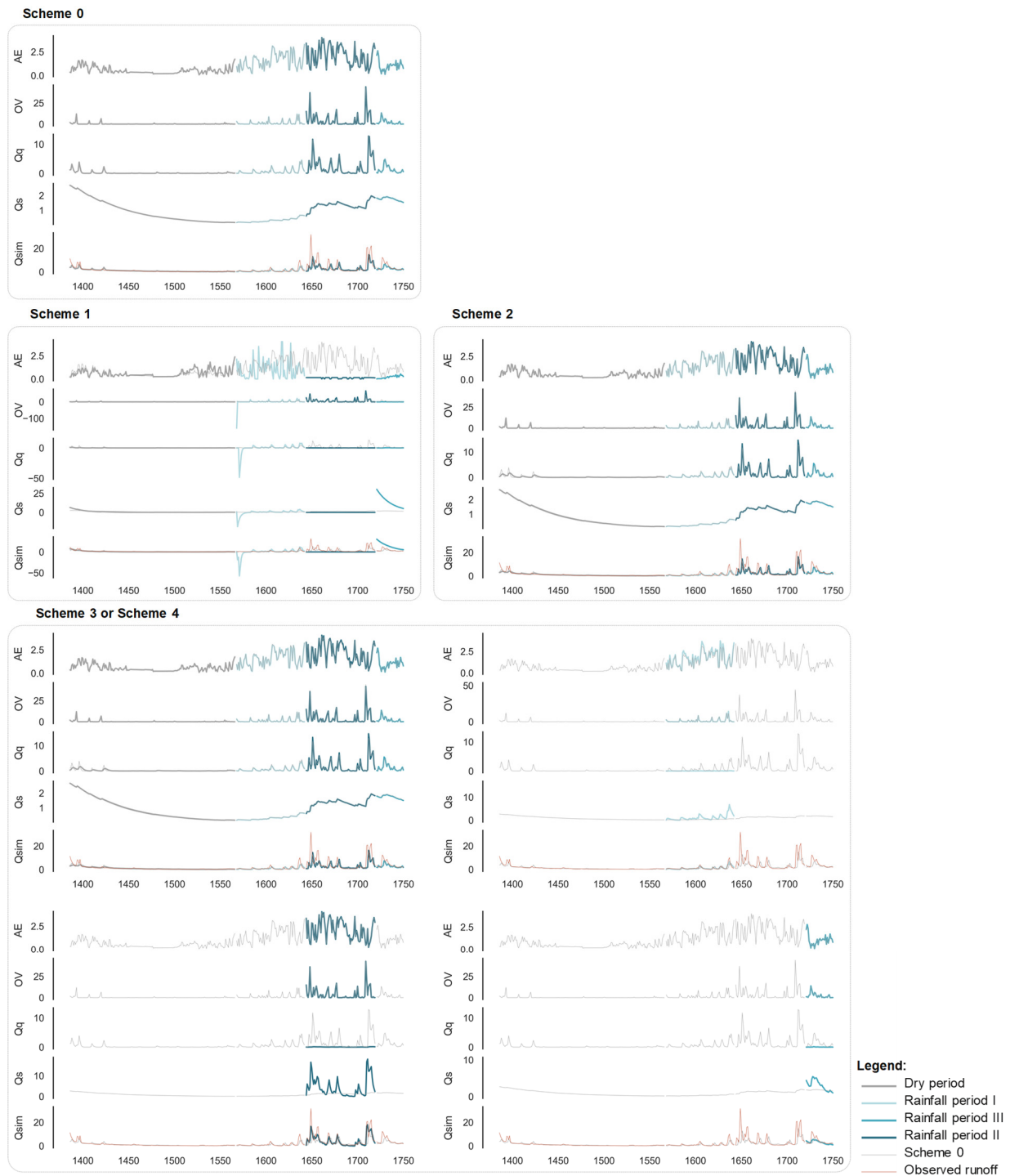


Figure S5. All fluxes (including AE , OV , Q_q , Q_s , and Q_{sim}) in a hydrological year for five schemes in the calibration period in Hanzhong basin. The thin grey lines denote the simulated fluxes time series in Scheme 0. The red lines denote the observed streamflow time series.

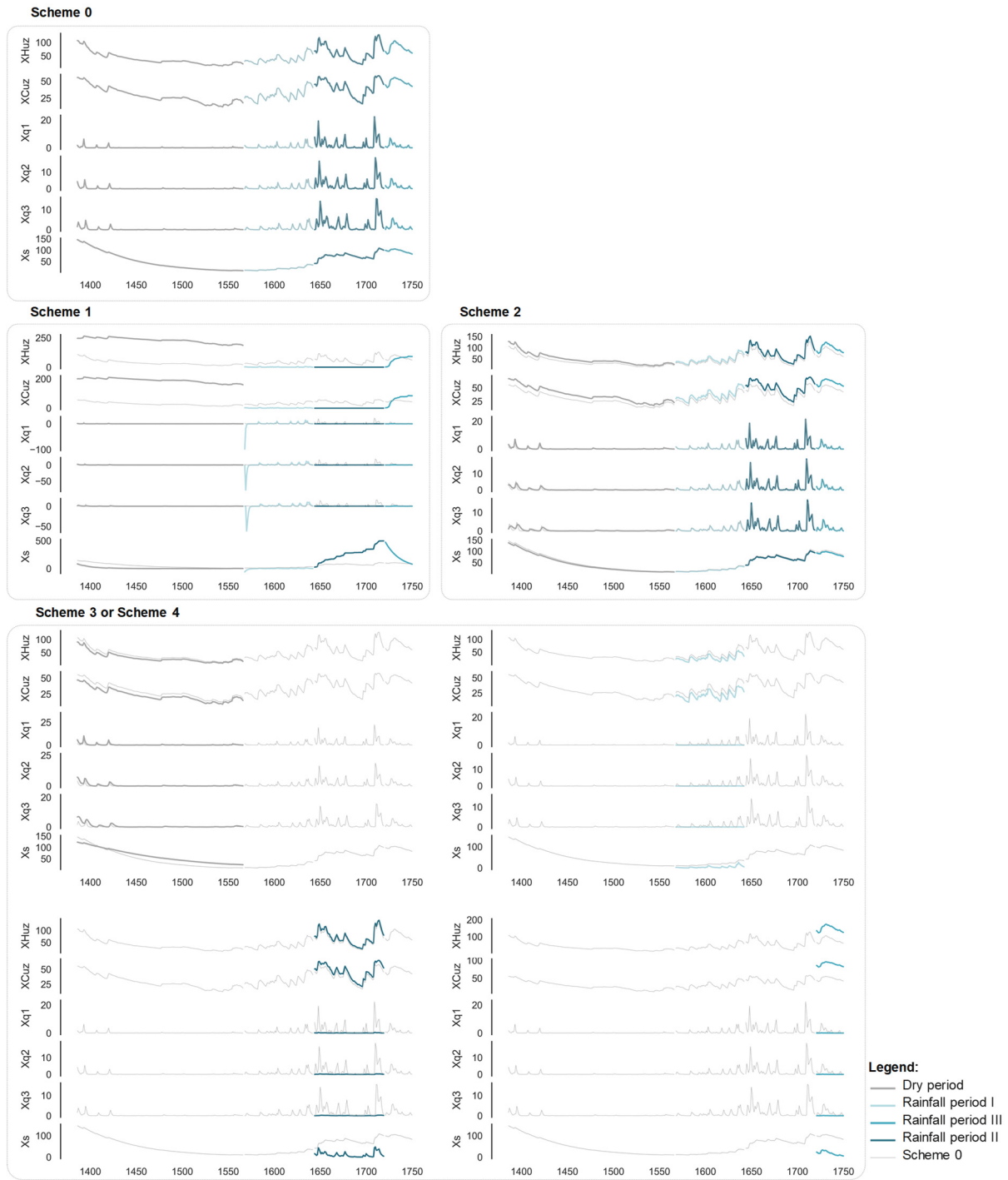


Figure S6. All state variables (including X_{Huz} , X_{Cuz} , X_{q1} , X_{q2} , X_{q3} , and X_s) in a hydrological year for five schemes in the calibration period in Hanzhong basin. The thin grey lines denote the simulated state variables time series in Scheme 0.

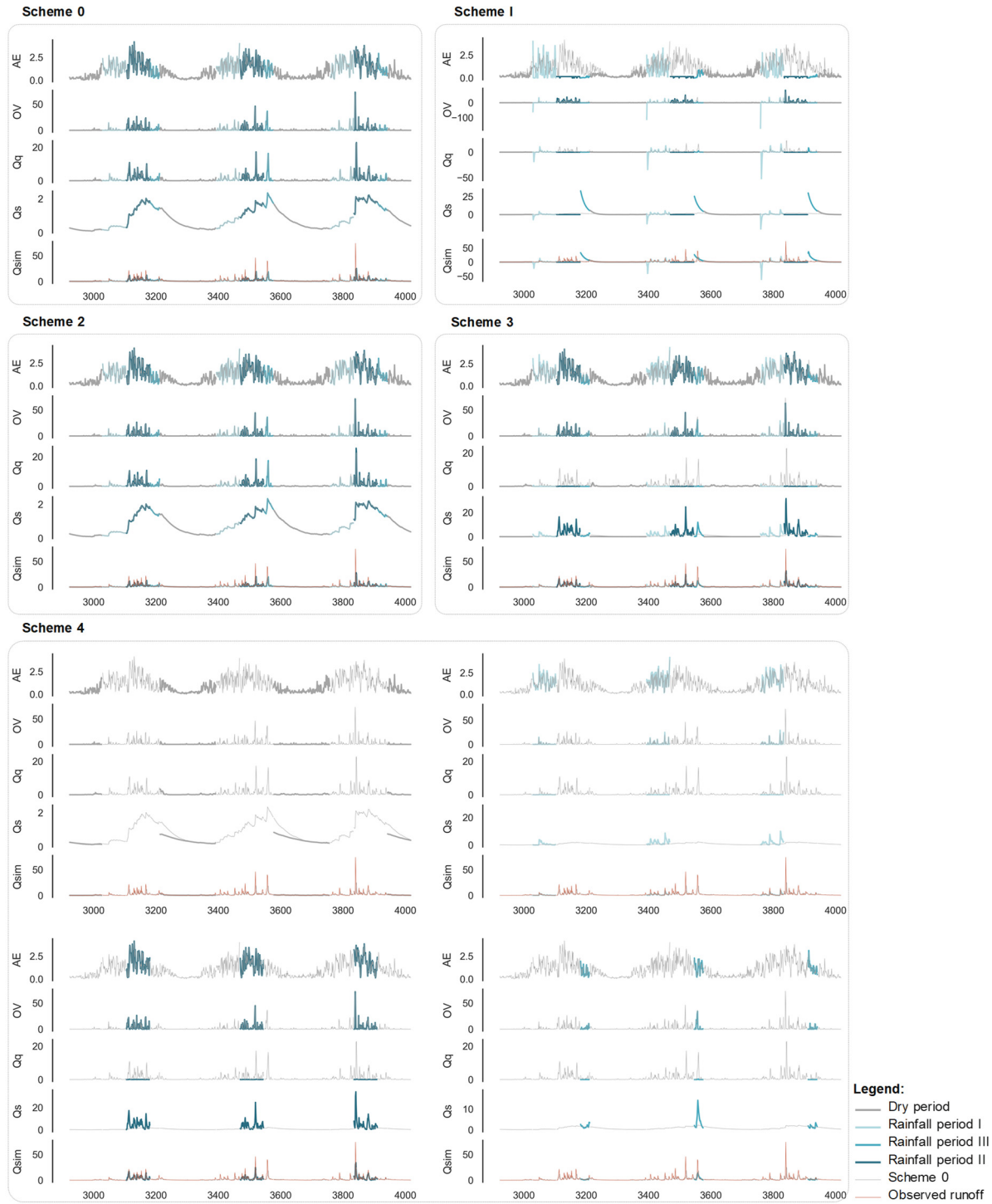


Figure S7. All fluxes (including AE , OV , Q_q , Q_s , and Q_{sim}) for five schemes in the whole verification period in Hanzhong basin. The thin grey lines denote the simulated fluxes time series in Scheme 0. The red lines denote the observed streamflow time series.

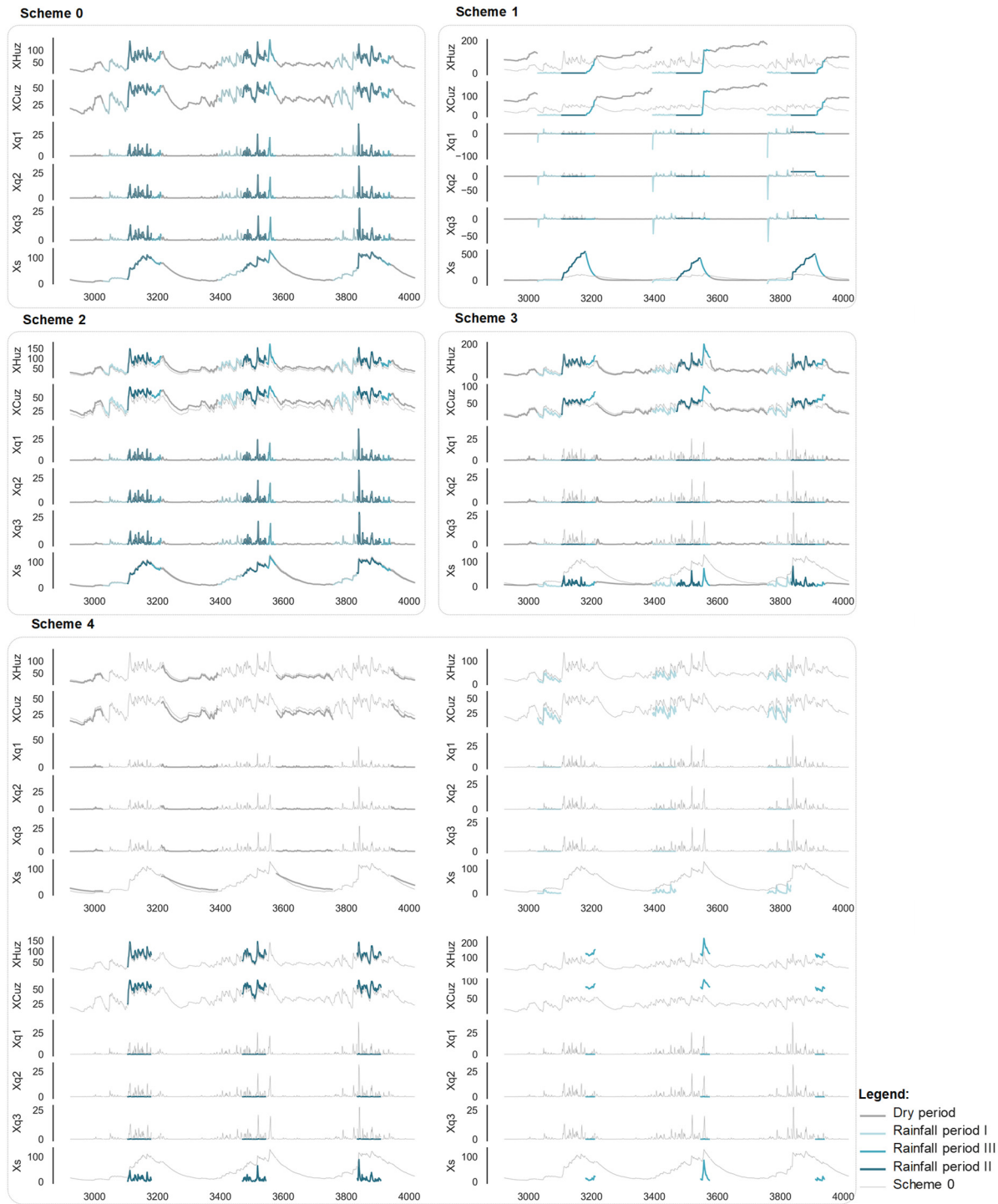


Figure S8. All state variables (including X_{Huz} , X_{Cuz} , X_{q1} , X_{q2} , X_{q3} , and X_s) for five schemes in the whole verification period in Hanzhong basin. The thin grey lines denote the simulated state variables time series in Scheme 0.

7 Convergence performance in Mumahe basin and Xunhe basin using ECP-VP

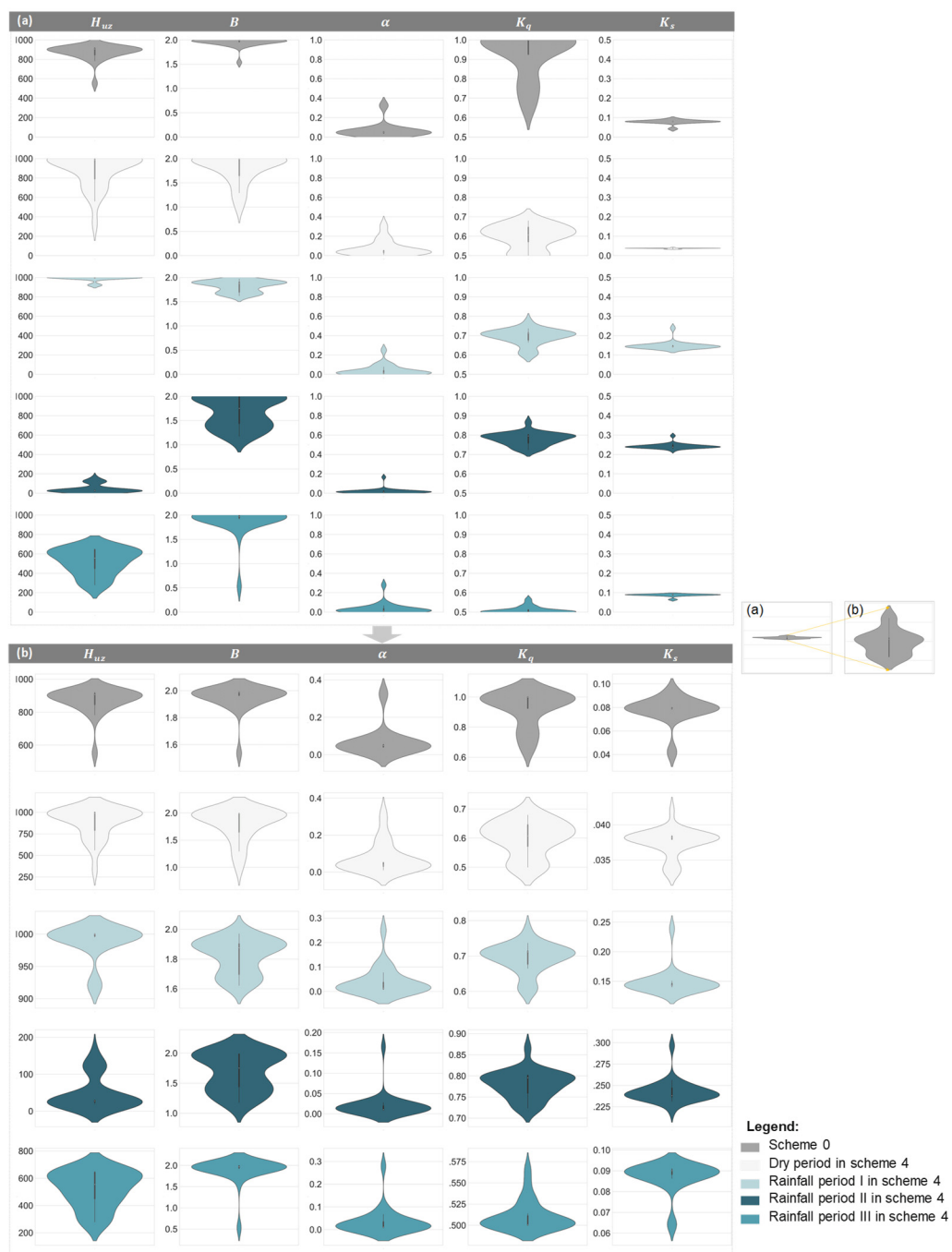


Figure S9. Convergence performance for Scheme 0 and Scheme 4 in individual parameter spaces in Mumahe basin using ECP-VP approach.

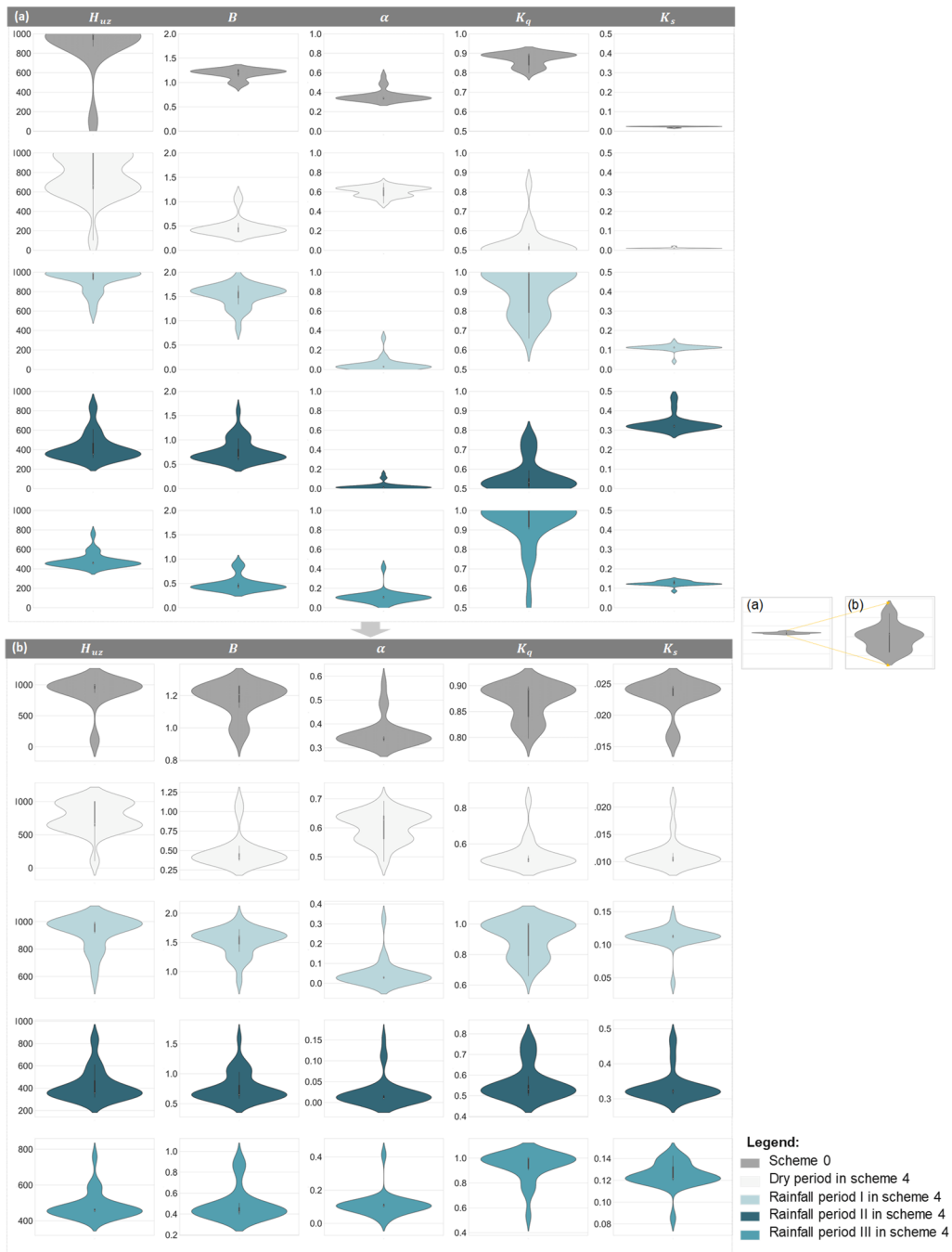


Figure S10. Convergence performance for Scheme 0 and Scheme 4 in individual parameter spaces in Xunhe basin using ECP-VP approach.

References

- Chen, K. L., Mei, J. J., Rehren, T., and Zhao, C. C.: Indigenous production and interregional exchange: late second-millennium BC bronzes from the Hanzhong basin, China, *Antiquity*, 90, 665-678, <https://doi.org/10.15184/aqy.2016.94>, 2016.
- Cheng, L., Yaeger, M., Viglione, A., Coopersmith, E., Ye, S., and Sivapalan, M.: Exploring the physical controls of regional patterns of flow duration curves – Part 1: Insights from statistical analyses, *Hydrol Earth Syst Sc*, 16, 4435-4446, 10.5194/hess-16-4435-2012, 2012.
- Coopersmith, E., Yaeger, M. A., Ye, S., Cheng, L., and Sivapalan, M.: Exploring the physical controls of regional patterns of flow duration curves – Part 3: A catchment classification system based on regime curve indicators, *Hydrol Earth Syst Sc*, 16, 4467-4482, 10.5194/hess-16-4467-2012, 2012.
- 10 De Vos, N. J., Rientjes, T. H. M., and Gupta, H. V.: Diagnostic evaluation of conceptual rainfall-runoff models using temporal clustering, *Hydrological Processes*, 24, 2840-2850, <https://doi.org/10.1002/hyp.7698>, 2010.
- Duan, Q. Y., Gupta, V. K., and Sorooshian, S.: Shuffled complex evolution approach for effective and efficient global minimization, *Journal of Optimization Theory and Applications*, 76, 501-521, 10.1007/bf00939380, 1993.
- Duan, Q. Y., Sorooshian, S., and Gupta, V. K.: Optimal use of the SCE-UA global optimization method for calibrating watersheds models, *J. Hydrol.*, 158, 265-284, [https://doi.org/10.1016/0022-1694\(94\)90057-4](https://doi.org/10.1016/0022-1694(94)90057-4) 1994.
- 15 Duan, Q., Sorooshian, S., and Gupta, V.: Effective and efficient global optimization for conceptual rainfall - runoff models, *Water Resources Research*, 28, 1015-1031, 10.1029/91WR02985, 1992.
- Eckhardt, K., and Arnold, J. G.: Automatic calibration of a distributed catchment model, *Journal of Hydrology*, 251, 103-109, [https://doi.org/10.1016/s0022-1694\(01\)00429-2](https://doi.org/10.1016/s0022-1694(01)00429-2), 2001.
- 20 Fang, J., Song, Y., Liu, H., and Piao, S.: Vegetation-climate relationship and its application in the division of vegetation zone in China, *Acta Botanica Sinica*, 44, 1105-1122, 2002.
- Hintze, J. L., and Nelson, R. D.: Violin plots: a box plot-density trace synergism, *The American Statistician*, 52, 181-184, <https://doi.org/10.2307/2685478>, 1998.
- Khakbaz, F., and Kazeminezhad, M.: Work hardening and mechanical properties of severely deformed AA3003 by constrained groove pressing, *Journal of Manufacturing Processes*, 14, 20-25, <https://doi.org/10.1016/j.jmapro.2011.07.001>, 2012.
- 25 Kim, D., and Kaluarachchi, J.: Predicting streamflows in snowmelt-driven watersheds using the flow duration curve method, *Hydrol Earth Syst Sc*, 18, 1679-1693, 10.5194/hess-18-1679-2014, 2014.
- Li, Z. J., Liu, P., Deng, C., Guo, S. L., He, P., and Wang, C. J.: Evaluation of Estimation of Distribution Algorithm to Calibrate Computationally Intensive Hydrologic Model, *J Hydrol Eng*, 21, 04016012, [https://doi.org/10.1061/\(asce\)he.1943-](https://doi.org/10.1061/(asce)he.1943-30)
- 30 5584.0001350, 2016.
- Lin, K. R., Zhang, Q., and Chen, X. H.: An evaluation of impacts of DEM resolution and parameter correlation on TOPMODEL modeling uncertainty, *J. Hydrol.*, 394, 370-383, <https://doi.org/10.1016/j.jhydrol.2010.09.012>, 2010.

- Moore, R. J.: The probability-distributed principle and runoff production at point and basin scales, *Hydrological Sciences Journal*, 30, 273-297, 10.1080/02626668509490989, 1985.
- Pathiraja, S., Anghileri, D., Burlando, P., Sharma, A., Marshall, L., and Moradkhani, H.: Time-varying parameter models for catchments with land use change: the importance of model structure, *Hydrol Earth Syst Sc*, 22, 2903-2919, 10.5194/hess-22-2903-2018, 2018.
- 5 Pfannerstill, M., Guse, B., and Fohrer, N.: Smart low flow signature metrics for an improved overall performance evaluation of hydrological models, *Journal of Hydrology*, 510, 447-458, <https://doi.org/10.1016/j.jhydrol.2013.12.044>, 2014.
- Pugliese, A., Castellarin, A., and Brath, A.: Geostatistical prediction of flow-duration curves in an index-flow framework, *Hydrol Earth Syst Sc*, 18, 3801-3816, 10.5194/hess-18-3801-2014, 2014.
- 10 Sorooshian, S., Duan, Q., and Gupta, V. K.: Calibration of rainfall - runoff models: Application of global optimization to the Sacramento Soil Moisture Accounting Model, *Water Resour. Res.*, 29, 1185-1194, <https://doi.org/10.1029/92wr02617>, 1993.
- Sun, X., Lu, H., Wang, S., and Yi, S.: Ages of Liangshan Paleolithic sites in Hanzhong Basin, central China, *Quat Geochronol*, 10, 380-386, <https://doi.org/10.1016/j.quageo.2012.04.014>, 2012.
- Vrugt, J. A., Bouten, W., Gupta, H. V., and Sorooshian, S.: Toward improved identifiability of hydrologic model parameters: The information content of experimental data, *Water Resources Research*, 38, 48-41-48-13, doi:10.1029/2001WR001118, 2002.
- 15 Wagener, T., Boyle, D. P., Lees, M. J., Wheater, H. S., Gupta, H. V., and Sorooshian, S.: A framework for development and application of hydrological models, *Hydrol. Earth Syst. Sci.*, 5, 13-26, 10.5194/hess-5-13-2001, 2001.
- Yadav, M., Wagener, T., and Gupta, H.: Regionalization of constraints on expected watershed response behavior for improved predictions in ungauged basins, *Advances in Water Resources*, 30, 1756-1774, <https://doi.org/10.1016/j.advwatres.2007.01.005>, 2007.
- 20